RIS Enabled Secure Communication with Covert Constraint

Ufuk Altun, Ertugrul Basar
Dept. of Electronics and Communication Engineering
Koç University
Istanbul, Turkey
ualtun20@ku.edu.tr, ebasar@ku.edu.tr

***Abstract*—Reconfigurable intelligent surface (RIS)-empowered communication is an emerging technology that is able to effectively reshape the wireless environment into the desired form. This promising technology appears as a remedy for a wide range of wireless applications including physical layer (PHY) security. In this paper, we consider the use of RISs for a challenging PHY security scenario with two kinds of adversaries, where a warden aims to detect and an eavesdropper aims to sniff the legitimate communication. Our objective is to maximize the secrecy rate under a covert constraint. For this purpose, a sub-optimal optimization algorithm is proposed where transmit beamforming and the RIS phase shift vectors are alternately optimized. The secrecy rate performance of the proposed algorithm is investigated with computer simulations for Rician fading channels. Our results indicate that the use of RISs significantly improves the secure communication rate of a wireless system without waking the warden.**

***Index Terms*—Alternating optimization, covert constraint, covertness, physical layer security, reconfigurable intelligent surface (RIS), secrecy rate.**

I. Introduction

RECONFIGURABLE intelligent surfaces (RISs) consist of multiple low-cost and passive electromagnetic wave reflection elements that are able to configure the phase of reflected signals. One of the important contributions of intelligent surfaces is that they can operate at a certain frequency without a power resource for signal processing (or require minimal energy in practice) due to their ideally passive nature. Moreover, they do not experience additional thermal noise, since they do not contain analog/digital converters or amplifiers [1]. These contributions motivated wireless communication researchers to control the wireless environment with RISs at strikingly low-costs. The main idea behind this approach is to direct the RIS-reflected signals at the desired point constructively or destructively. Since the reflection phases of RISs are dynamically controllable, the channel response of a wireless link can be adjusted with the RIS-reflected signals. Based on this, intelligent surfaces gained massive attention and are proposed for a wide range of wireless applications from localization to edge computing [2], [3].

An important application of RISs is physical layer security. Since RISs are able to direct their reflected signals, they can be optimized to enhance the legitimate channel's capacity while weakening the adversary's. The main challenge of RIS aided security models is the optimization of certain system parameters [4]. In [5], optimization of transmit beamforming and RIS phase shifts are considered for non-line-of-sight (NLOS) channels where the transmitter and the receiver are only connected over the RIS channel. The authors propose an algorithm to maximize the secrecy rate for the scenario where only the transmitter is equipped with multiple antennas. In [6], the secrecy rate maximization problem is considered for the models with both direct and over-RIS channels. In [7], the eavesdropper is also equipped with multiple antennas. The case of multiple legitimate receivers and multiple eavesdroppers is considered in [8]. The addition of artificial noise to the transmitted signal is considered in [9]. In [10], system parameters are optimized to minimize the consumed transmit power under a secrecy constraint, instead of maximizing the secrecy rate. The scenario of multiple antennas is considered in [11]. Non-ideal cases such as imperfect channel state information (CSI) or no CSI is considered in [12] and [13] respectively.

It should be noted that previously mentioned physical layer security models are based on degrading the eavesdropper's channel where the adversary is already aware of legitimate communication. These models can be insufficient against advanced adversary models where the attacker can take additional actions. Moreover, the purpose of the attack, in some cases, might be to detect the communication instead of eavesdropping. Covert communication is another physical layer application that targets these scenarios where the objective is to communicate without being detected by the adversary [14], [15]. Implementation of RIS is also considered for covert communication in [16]–[19] to improve the covert communication rate. Both adversary models (an eavesdropper and a warden) in the same scenario has been considered in the literature where an eavesdropper aims to sniff and a warden aims to detect the legitimate communication [20]–[23]. However, the implementation of intelligent surfaces and their parameter optimization for this attack model is an open issue.

In this paper, we consider an RIS enabled secure communication scheme against the mixed adversary model with an eavesdropper and a warden. In this scenario, we aim to optimize the transmit beamforming and the RIS phase shifts to maximize the secrecy rate. Contrary to the previous studies, our attacker model introduces a received power constraint to the optimization problem, which is very difficult to solve in

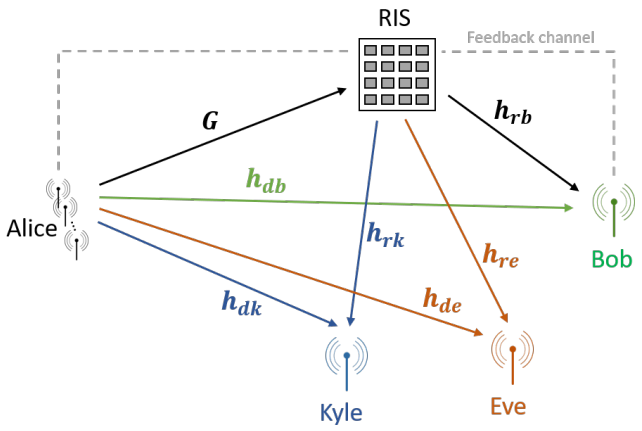


Fig. 1. A wireless MISO scheme where Alice communicates with Bob with the help of an RIS link. Alice aims to send information to Bob without being detected by Kyle and without leaking information to Eve.

closed-form. Our main contribution is that we propose an algorithm to effectively solve this optimization problem where the secrecy rate is maximized under the covert constraint. [1] Circularly symmetric complex Gaussian distribution with zero mean and σ^2 variance is denoted by $\mathcal{CN}(0, \sigma^2)$.

II. System Model

Consider a point-to-point communication scenario where a transmitter (Alice) aims to communicate with a receiver (Bob) with the help of an RIS link as depicted in Fig. 1. In the meantime, Kyle aims to detect and Eve aims to eavesdrop the legitimate communication. It is assumed that Alice and RIS are equipped with M antennas and N reflecting elements respectively, while Bob, Kyle and Eve have a single antenna. In order to prevent Kyle and Eve from detecting and sniffing the communication respectively, Alice is able to control the beamforming vector of its antennas and the phase shifts of RIS reflecting elements.

The channel coefficient vectors of Alice-Bob, Alice-Kyle and Alice-Eve direct links are denoted by $\boldsymbol{h}_{db} \in \mathbb{C}^{M\times 1}$, $\boldsymbol{h}_{dk} \in \mathbb{C}^{M\times 1}$ and $\boldsymbol{h}_{de} \in \mathbb{C}^{M\times 1}$, respectively. The channel coefficient vectors of RIS-Bob, RIS-Kyle and RIS-Eve over-RIS reflection links are denoted by $\boldsymbol{h}_{rb} \in \mathbb{C}^{N\times 1}$, $\boldsymbol{h}_{rk} \in \mathbb{C}^{N\times 1}$ and $\boldsymbol{h}_{re} \in \mathbb{C}^{N\times 1}$, respectively. The channel coefficient matrix of Alice-RIS link is denoted by $\boldsymbol{G} \in \mathbb{C}^{N\times M}$. RISs are known to be effectively configurable to work in receiving and reflecting modes. Hence, we assume that Alice can obtain both direct and over-RIS channel coefficients by observing wireless environment (as in [6], [9], [24]).

Alice essentially configures its transmit beamforming vector $\boldsymbol{w} \in \mathbb{C}^{M\times 1}$ and RIS phase shift vector $\boldsymbol{\theta} \in \mathbb{C}^{1\times N}$ to secure its communication. The transmit beamforming vector is bounded by the maximum power constraint as,

$$||\boldsymbol{w}||^2 \leq P_m. \tag{1}$$

The RIS phase shift vector can be defined as,

$$\boldsymbol{\theta} = [\beta_1 e^{j\theta_1}, \ldots, \beta_n e^{j\theta_n}, \ldots, \beta_N e^{j\theta_N}], \tag{2}$$

where $\beta_n \in [0, 1]$ is the reflection amplitude and $\theta_n \in [0, 2\pi)$ is the phase shift of the n^{th} reflecting element. The reflection amplitudes are selected as $\beta_n = 1, \forall n$ throughout the paper to attain maximum reflection gain. Considering both direct and over-RIS links, the received signals at Bob, Eve and Kyle can be given as follows.

$$y_i = (\boldsymbol{h}_{ri}^H \boldsymbol{\Theta} \boldsymbol{G} + \boldsymbol{h}_{di}^H)\boldsymbol{w}s + n_i, \qquad i \in \{b, e, k\} \tag{3}$$

Here, $\boldsymbol{\Theta} = \text{diag}(\boldsymbol{\theta})$ is the diagonal matrix of phase shifts $\boldsymbol{\theta}$. The thermal noise terms at Bob, Eve and Kyle are denoted by $n_b \sim \mathcal{CN}(0, \sigma_b^2)$, $n_e \sim \mathcal{CN}(0, \sigma_e^2)$ and $n_k \sim \mathcal{CN}(0, \sigma_k^2)$, respectively. The main performance metric of the study is the secrecy rate which can be defined as,

$$R_{sec} = \max(R_b - R_e), \tag{4}$$

where R_b and R_e are the achievable rates of Alice-Bob and Alice-Eve channels as,

$$R_i = \log_2\left(1 + \frac{|(\boldsymbol{h}_{ri}^H \boldsymbol{\Theta} \boldsymbol{G} + \boldsymbol{h}_{di}^H)\boldsymbol{w}|^2}{\sigma_i^2}\right), \qquad i \in \{b, e\} \tag{5}$$

The objective of Kyle is to detect the transmission by using a detection mechanism. Traditionally, the sum of false alarm and missed detection probabilities ($\xi = P_{FA} + P_{MD}$) of Kyle's detection mechanism is used to examine covertness. For a given ξ, it is shown that a received power threshold (Γ) at Kyle can be defined to satisfy the inequality of $\xi \leq 1 - \epsilon$ where ϵ is an arbitrarily small value [14]. Hence, we can define the covert constraint with a received power threshold at Kyle as,

$$|(\boldsymbol{h}_{rk}^H \boldsymbol{\Theta} \boldsymbol{G} + \boldsymbol{h}_{dk}^H)\boldsymbol{w}|^2 < \Gamma. \tag{6}$$

Alice essentially aims to maximize the secrecy rate in (4) without violating the maximum power constraint in (1) and the covert constraint in (6). For this purpose, Alice aims to optimize its transmit beamforming and RIS phase shifts. The optimization problem in hand can be given as,

$$\begin{aligned}
(\text{P1}): \max_{\boldsymbol{w},\boldsymbol{\theta}} \; & \log_2\left(1 + \frac{|(\boldsymbol{h}_{rb}^H \boldsymbol{\Theta} \boldsymbol{G} + \boldsymbol{h}_{db}^H)\boldsymbol{w}|^2}{\sigma_b^2}\right) \\
& - \log_2\left(1 + \frac{|(\boldsymbol{h}_{re}^H \boldsymbol{\Theta} \boldsymbol{G} + \boldsymbol{h}_{de}^H)\boldsymbol{w}|^2}{\sigma_e^2}\right) && \text{(7a)} \\
\text{s.t.} \quad & ||\boldsymbol{w}||^2 \leq P_m && \text{(7b)} \\
& \beta_n = 1, \forall n && \text{(7c)} \\
& |(\boldsymbol{h}_{rk}^H \boldsymbol{\Theta} \boldsymbol{G} + \boldsymbol{h}_{dk}^H)\boldsymbol{w}|^2 < \Gamma. && \text{(7d)}
\end{aligned}$$

It should be noted that the objective function of (P1) is a non-concave function (for both $\boldsymbol{w}$ and $\boldsymbol{\theta}$) which is not straightforward to maximize. For this reason, the following section is dedicated to the sub-optimal solution of (P1) with alternating optimization (AO).

[1] Throughout the paper, lowercase and uppercase boldface characters are used to represent vectors and matrices, respectively. A column vector $\boldsymbol{x} \in \mathbb{C}^{a\times 1}$ and a raw vector $\boldsymbol{y} \in \mathbb{C}^{1\times a}$ are in a dimensional complex space. A matrix $\boldsymbol{X} \in \mathbb{C}^{a\times b}$ is in the space of $a \times b$ size complex valued matrices. Transpose, conjugate, conjugate transpose and trace of a matrix $\boldsymbol{X}$ is denoted by $\boldsymbol{X}^T$, $\boldsymbol{X}^*$, $\boldsymbol{X}^H$ and tr($\boldsymbol{X}$), respectively. $||\boldsymbol{x}||$ and $\hat{\boldsymbol{x}}$ represent the Euclidean norm of $\boldsymbol{x}$ and the unit vector of $\boldsymbol{x}$, respectively.

III. Proposed Approach

In this section, we present our solution that is based on alternately solving (P1) for either $\boldsymbol{w}$ or $\boldsymbol{\theta}$ while the other one is kept constant. It should be noted that the covert constraint and the received power at Kyle depend on both direct (Alice-Kyle) and over-RIS (Alice-RIS-Kyle) channels. While the optimization of $\boldsymbol{\theta}$ affects only the over-RIS channel, the optimization of $\boldsymbol{w}$ can directly affect both channels. As a result, the optimization of $\boldsymbol{\theta}$ is not enough to satisfy the covert constraint. However, the received power at Kyle can be completely controlled with $\boldsymbol{w}$. Based on this concept, we aim to reduce the complexity by dropping the covert constraint for the optimization of $\boldsymbol{\theta}$. Instead, a sub-optimal, yet less complex solution is obtained by satisfying the covert constraint only with $\boldsymbol{w}$.

A. Optimization of $\boldsymbol{\theta}$ with given $\boldsymbol{w}$

Since logarithm is a strictly increasing function, (P1) can be rearranged for a constant $\boldsymbol{w}$ as,

$$\text{(P2)}: \max_{\boldsymbol{\theta}} \ \frac{1+|(\boldsymbol{h}_{rb}^H\boldsymbol{\Theta}\boldsymbol{G}+\boldsymbol{h}_{db}^H)\boldsymbol{w}|^2\frac{1}{\sigma_b^2}}{1+|(\boldsymbol{h}_{re}^H\boldsymbol{\Theta}\boldsymbol{G}+\boldsymbol{h}_{de}^H)\boldsymbol{w}|^2\frac{1}{\sigma_e^2}} \tag{8a}$$

$$\text{s.t.} \quad \beta_n = 1, \forall n. \tag{8b}$$

Here, the covert constraint is dropped to reduce the computational complexity. Solution to (P2) has been presented in the literature [6] and uses the following auxiliary variables to transform (P2) into a solvable form.

$$\boldsymbol{G}_i = \frac{1}{\sigma_i^2}\begin{bmatrix}\text{diag}(\boldsymbol{h}_{ri})\boldsymbol{G}^*\boldsymbol{w}^*\boldsymbol{w}^{*T}\boldsymbol{G}^T\text{diag}(\boldsymbol{h}_{ri}^H) & \text{diag}(\boldsymbol{h}_{ri})\boldsymbol{G}^*\boldsymbol{w}^*\boldsymbol{w}^{*T}\boldsymbol{h}_{di}^* \\ \boldsymbol{h}_{di}^T\boldsymbol{w}^*\boldsymbol{w}^{*T}\boldsymbol{G}^T\text{diag}(\boldsymbol{h}_{ri}^H) & 0\end{bmatrix}$$

$$H_i = \boldsymbol{h}_{di}^T\boldsymbol{w}^*\boldsymbol{w}^T\boldsymbol{h}_{di}^*\frac{1}{\sigma_i^2}, \qquad i \in \{b, e\}$$

$$\boldsymbol{E}_n = \begin{bmatrix} e_{11} & \cdots & e_{1N} \\ \vdots & \ddots & \vdots \\ e_{N1} & \cdots & e_{NN}\end{bmatrix} = \begin{cases} e_{ij} = 1 & \text{if } i = j = n \\ e_{ij} = 0 & \text{otherwise}\end{cases}$$

$$\boldsymbol{s} = \begin{bmatrix}\boldsymbol{\theta} & 1\end{bmatrix}^T$$

After substituting the auxiliary variables into (P2), we can transform our optimization problem into the form of,

$$\text{(P3)}: \max_{\boldsymbol{s}} \ \frac{1+\boldsymbol{s}^H\boldsymbol{G}_b\boldsymbol{s}+H_b}{1+\boldsymbol{s}^H\boldsymbol{G}_e\boldsymbol{s}+H_e} \tag{10a}$$

$$\text{s.t.} \quad \boldsymbol{s}^H\boldsymbol{E}_n\boldsymbol{s} = 1, \forall n. \tag{10b}$$

The resulting problem is still directly not solvable since the objective function is non-concave and fractional. However, (P3) is now suitable to relaxation to overcome its non-concavity [25]. The change of variables $\boldsymbol{S} = \boldsymbol{s}\boldsymbol{s}^H$ is applied to express the optimization problem in the equivalent form,

$$\text{(P4)}: \max_{\boldsymbol{S}\succeq 0} \ \frac{1+\text{tr}(\boldsymbol{G}_b\boldsymbol{S})+H_b}{1+\text{tr}(\boldsymbol{G}_e\boldsymbol{S})+H_e} \tag{11a}$$

$$\text{s.t.} \quad \text{tr}(\boldsymbol{E}_n\boldsymbol{S}) = 1, \forall n. \tag{11b}$$

Initially, the definition of $\boldsymbol{S}$ requires $S \succeq 0$ and rank($\boldsymbol{S}$) $= 1$ conditions. Since rank($\boldsymbol{S}$) $= 1$ constraint is non-convex, it is removed in (P4) to relax the optimization problem. Lastly, by applying the change of variables $\mu = 1/1+\text{tr}(\boldsymbol{G}_e\boldsymbol{S})+H_e$ and $\boldsymbol{X} = \mu\boldsymbol{S}$, (P4) can be represented without fraction as [6],

$$\text{(P5)}: \max_{\boldsymbol{X}\succeq 0,\mu\geq 0} \ \text{tr}(\boldsymbol{G}_e\boldsymbol{X})+\mu(H_e+1) \tag{12a}$$

$$\text{s.t.} \quad \text{tr}(\boldsymbol{G}_b\boldsymbol{X})+\mu(H_b+1) = 1 \tag{12b}$$

$$\text{tr}(\boldsymbol{E}_n\boldsymbol{X}) = \mu, \forall n \tag{12c}$$

Notice that (P5) is a convex semidefinite program (SDP) and can be solved by convex programming solvers such as CVX. However, (P5) is a relaxed form of (P3) and ignores the rank-1 constraint. As a result, rank-1 solutions to (P5) are constructed by Gaussian optimization as follows.

Firstly, $\boldsymbol{X}$ is decomposed into its diagonal matrix of eigenvalues $\boldsymbol{D} \in \mathbb{C}^{(N+1)\times(N+1)}$ and corresponding eigenvectors $\boldsymbol{V} \in \mathbb{C}^{(N+1)\times(N+1)}$. Then, a sub-optimal solution to (P3) is constructed by

$$\boldsymbol{s} = \boldsymbol{V}\boldsymbol{D}^{\frac{1}{2}}\boldsymbol{r}, \tag{13}$$

where $\boldsymbol{r} \in \mathbb{C}^{(N+1)\times 1} \sim \mathcal{CN}(0, \boldsymbol{I}_{N+1})$ is a random vector. After generating multiple solutions with multiple $\boldsymbol{r}$ vectors by using (13); the solution that maximizes the objective function of (P3) is selected as the best solution. Lastly, the solution of (P2) can be obtained by reconstructing $\boldsymbol{\theta}$ from,

$$\boldsymbol{\theta} = \tilde{\boldsymbol{s}}/s_{N+1}. \tag{14}$$

where $\tilde{\boldsymbol{s}}$ indicates the vector which is formed by the first N elements of $\boldsymbol{s}$ and s_{N+1} denotes the $(N+1)^{\text{th}}$ element of $\boldsymbol{s}$. The resulting phase shifts maximize the RIS-Bob channel while minimizing RIS-Eve channel for a constant $\boldsymbol{w}$. Although Kyle's channel is not considered in $\boldsymbol{\theta}$, the received power at Kyle is kept under the threshold with the optimization of $\boldsymbol{w}$ as follows.

B. Optimization of $\boldsymbol{w}$ with given $\boldsymbol{\theta}$

After obtaining the phase shift vector, the transmit beamforming vector can be optimized by considering $\boldsymbol{\theta}$ as a constant. The proposed approach is based on projecting both Alice-Bob and Alice-Kyle channels into the null space of the Alice-Eve channel [26]. Since Eve's channel is nullified with the projection, the problem becomes the maximization of Bob's channel under covert constraint. Since $\boldsymbol{\theta}$ is constant, direct and over-RIS channels can be rearranged as,

$$\boldsymbol{h}_i = (\boldsymbol{h}_{ri}^H\boldsymbol{\Theta}\boldsymbol{G}+\boldsymbol{h}_{di}^H)^H, \qquad i \in \{b, e, k\}. \tag{15}$$

Using a change of variable in (15), Bob and Kyle's channels can be projected to zero-force Eve's channel as,

$$\boldsymbol{h}_i^\perp = (\boldsymbol{I}_M - \hat{\boldsymbol{h}}_e\hat{\boldsymbol{h}}_e^H)\boldsymbol{h}_i, \qquad i \in \{b, k\}, \tag{16}$$

where $\boldsymbol{h}_b^\perp$ and $\boldsymbol{h}_k^\perp$ are Bob's and Kyle's projected channels, respectively, that are perpendicular to Eve's channel. As a

Algorithm 1: Sub-optimal algorithm for secrecy rate maximization with covert constraint.

Initialization: Set the maximum number of iterations K, the threshold ϵ, iteration counter $k = 1$, transmit beamforming vector $\boldsymbol{w}^{(k)} = \sqrt{P_m}\hat{\boldsymbol{h}}_b$ and RIS phase shift vector $\boldsymbol{\theta}^{(k)} = [1, \ldots, 1]^{1,N}$.

repeat

Calculate RIS phase shift vector $\boldsymbol{\theta}^{(k)}$ by solving (P5) and applying Gaussian randomization in (13) and (14) with given $\boldsymbol{w}^{(k)}$.

Calculate transmit beamforming vector $\boldsymbol{w}^{(k)}$ by using (18).

Set $k = k + 1$.

until;

$k = K$

result, the optimization problem can be simplified as a rate maximization problem with covert constraint as:

$$\text{(P7)}: \max_{\boldsymbol{w}} \ \boldsymbol{w}^H \boldsymbol{B} \boldsymbol{w} \tag{17a}$$

$$\text{s.t.} \quad \boldsymbol{w}^H \boldsymbol{w} \leq P_m \tag{17b}$$

$$\boldsymbol{w}^H \boldsymbol{K} \boldsymbol{w} < \Gamma, \tag{17c}$$

where $\boldsymbol{B} = \boldsymbol{h}_b^{\perp} \boldsymbol{h}_b^{\perp H} \frac{1}{\sigma_b^2}$ and $\boldsymbol{K} = \boldsymbol{h}_k^{\perp} \boldsymbol{h}_k^{\perp H}$. Solution to (P7) can be expressed as a linear combination of maximum-ratio-transmission (MRT) beamforming and zero-forcing (ZF) beamforming as [26],

$$\boldsymbol{w} = \sqrt{P_m} \left(\alpha \hat{\boldsymbol{h}}_k^{\perp} + \beta (\boldsymbol{I} - \hat{\boldsymbol{h}}_k^{\perp} (\hat{\boldsymbol{h}}_k^{\perp})^H) \hat{\boldsymbol{h}}_b^{\perp} \right), \tag{18}$$

where α and β are,

$$\alpha = \begin{cases} \frac{(\hat{\boldsymbol{h}}_k^{\perp})^H \boldsymbol{h}_b^{\perp}}{||\boldsymbol{h}_b^{\perp}||}, & \text{if } P_m ||\boldsymbol{h}_k^{\perp}||^2 \left(\frac{|(\hat{\boldsymbol{h}}_k^{\perp})^H \boldsymbol{h}_b^{\perp}|}{||\boldsymbol{h}_b^{\perp}||} \right)^2 \leq \Gamma \\ \lambda \left(\frac{(\hat{\boldsymbol{h}}_k^{\perp})^H \boldsymbol{h}_b^{\perp}}{||(\hat{\boldsymbol{h}}_k^{\perp})^H \boldsymbol{h}_b^{\perp}||} \right), & \text{otherwise} \end{cases} \tag{19a}$$

$$\beta = \begin{cases} \frac{((\boldsymbol{I} - \hat{\boldsymbol{h}}_k^{\perp} (\hat{\boldsymbol{h}}_k^{\perp})^H) \hat{\boldsymbol{h}}_b^{\perp})^H \boldsymbol{h}_b^{\perp}}{||\boldsymbol{h}_b^{\perp}||}, & \text{if } P_m ||\boldsymbol{h}_k^{\perp}||^2 \left(\frac{|(\hat{\boldsymbol{h}}_k^{\perp})^H \boldsymbol{h}_b^{\perp}|}{||\boldsymbol{h}_b^{\perp}||} \right)^2 \leq \Gamma \\ \sqrt{1 - \lambda^2} \left(\frac{((\boldsymbol{I} - \hat{\boldsymbol{h}}_k^{\perp} (\hat{\boldsymbol{h}}_k^{\perp})^H) \hat{\boldsymbol{h}}_b^{\perp})^H \boldsymbol{h}_b^{\perp}}{||((\boldsymbol{I} - \hat{\boldsymbol{h}}_k^{\perp} (\hat{\boldsymbol{h}}_k^{\perp})^H) \hat{\boldsymbol{h}}_b^{\perp})^H \boldsymbol{h}_b^{\perp}||} \right), & \text{otherwise} \end{cases} \tag{19b}$$

and $\lambda = \sqrt{\frac{\Gamma}{P_m ||\boldsymbol{h}_k^{\perp}||^2}}$. By zero-forcing Eve, the method guarantees that Eve's channel is nullified; hence, maximizing Bob's rate also maximizes the secrecy rate. The complete algorithm that alternately optimizes $\boldsymbol{\theta}$ and $\boldsymbol{w}$ is given in Algorithm 1.

IV. Numerical Results

In this section, the feasibility of the proposed algorithm is examined with computer simulations. The simulation setup consists of Alice, Bob, RIS, Eve and Kyle at locations A$(0, 0)$, B$(150, 0)$, R$(145, 5)$, E$(145, 0)$ and K$(145, -5)$ in meters, respectively. The wireless channel is modeled as,

$$\boldsymbol{h}_i = \sqrt{L_0^{-1} \left(\frac{d_i}{d_0} \right)^{-c_i}} \left(\sqrt{\frac{\Omega_i}{\Omega_i + 1}} \boldsymbol{h}_{\text{LOS}} + \sqrt{\frac{1}{\Omega_i + 1}} \boldsymbol{h}_{\text{NLOS}} \right), \tag{20}$$

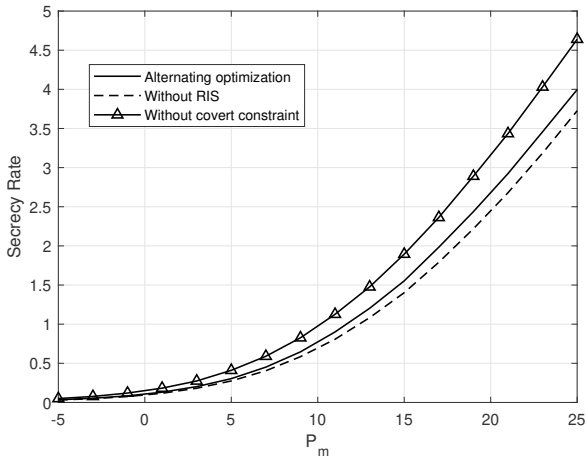
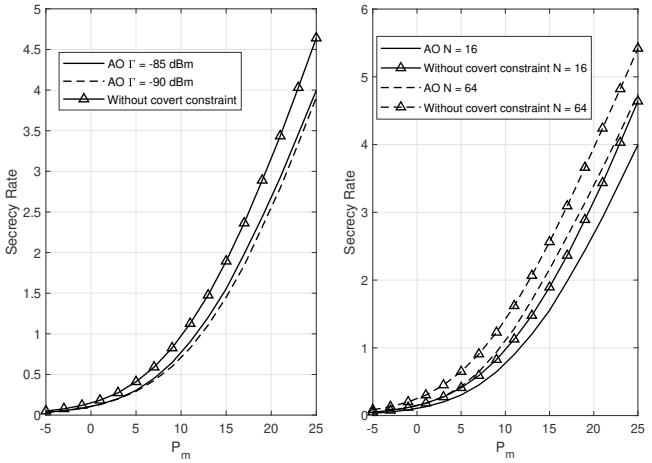


Fig. 2. The secrecy rate performance of Algorithm 1 for $M = 4$ transmit antennas and $N = 16$ RIS elements ($\Gamma = -85$ dBm).

for $i \in \{rb, re, rk, db, de, dk\}$, where $\boldsymbol{h}_{\text{LOS}}$ and $\boldsymbol{h}_{\text{NLOS}}$ indicate line-of-sight and non-line-of-sight channel components, respectively. The path loss at reference distance is $L_0 = 30$ dB and the reference distance is $d_0 = 1$ m. Path loss exponents are selected as $c_i = 3$ and Rician factors are selected as $\Omega_i = 1$ for $i \in \{rb, re, rk, db, de, dk\}$. Thermal noise powers at Bob and Eve are selected as $\sigma_b^2 = \sigma_e^2 = -80$ dBm. Computer simulations are repeated for 10^4 iterations. For each iteration, the number of alternating optimization iterations are set as $K = 3$.

The secrecy rate performance of the proposed approach is illustrated in Fig. 2. This figure shows the comparison of RIS enabled and without RIS cases for various transmit power constraints (P_m). $\boldsymbol{w}$ and $\boldsymbol{\theta}$ of the RIS enabled case are optimized with the proposed alternating optimization approach in Algorithm 1. In the traditional (without RIS) case, Bob, Eve and Kyle received signals directly from Alice, hence only $\boldsymbol{w}$ is optimized using (18). Also, an upper bound for the RIS enabled case is considered by removing the covert constraint. In this case, $\boldsymbol{w}$ and $\boldsymbol{\theta}$ are optimized with the alternating optimization algorithm given in [6] which considers only eavesdropping attack. The setup in Fig. 2 consists of $M = 4$ antennas at Alice, $N = 16$ reflecting elements at RIS and a $\Gamma = -85$ dBm received power constraint at Kyle. The first observation from this figure is that increasing the transmit power increases the achievable secrecy rate for all cases. Moreover, adding covert constraint degrades the secrecy rate for both RIS enabled and RIS disabled cases. The main result of Fig. 2 is that the application of RIS improves the secrecy rate of a wireless system against dual attacks where both an eavesdropper and a warden exist.

The impacts of the covert constraint and the number of RIS elements are investigated in Fig. 3. In Fig. 3(a), the covert constraint Γ is decreased from -85 dBm to -90 dBm, which reduces the allowed power level at Kyle without being detected. It can be observed that lower power levels reduce



(a) (b)

Fig. 3. The impact of covert constraint and the number of RIS elements to the performance of Algorithm 1. (a) For $\Gamma = -85, -90$ dBm ($M = 4$, $N = 16$). (b) For $N = 16, 64$ ($M = 4$, $\Gamma = -85$ dBm).

the secrecy rate of the system. The impact of the number of RIS elements is illustrated in Fig. 3(b). The results show that the secrecy rate with covert constraint can be improved with by increasing the number of reflecting elements at RIS.

V. Conclusion

We have considered the optimization problem of RIS enabled communication systems against an eavesdropper and a warden. The transmit beamforming and RIS phase shift vectors have been alternately optimized to maximize the secrecy rate under the covert constraint. We have considered two methods for the problem. In the first approach, the covert constraint is satisfied by nullifying Kyle's channel with transmit beamforming. In the second approach, Eve's channel is zero-forced and Bob's rate is maximized under the covert constraint. Lastly, the feasibility of the proposed approaches has been proved with numerical results where the addition of RIS improved the secrecy rate under the covert constraint.

References

[1] E. Basar, M. Di Renzo, J. De Rosny, M. Debbah, M.-S. Alouini, and R. Zhang, "Wireless Communications Through Reconfigurable Intelligent Surfaces," *IEEE Access*, vol. 7, no. June 2018, pp. 116 753–116 773, 2019.

[2] Q. Wu, S. Zhang, B. Zheng, C. You, and R. Zhang, "Intelligent Reflecting Surface Aided Wireless Communications: A Tutorial," vol. 999078, pp. 1–74, 2020.

[3] S. Gong, X. Lu, D. T. Hoang, D. Niyato, L. Shu, D. I. Kim, and Y. C. Liang, "Toward Smart Wireless Communications via Intelligent Reflecting Surfaces: A Contemporary Survey," *IEEE Communications Surveys and Tutorials*, vol. 22, no. 4, pp. 2283–2314, 2020.

[4] H. Shen, W. Xu, S. Gong, Z. He, and C. Zhao, "Secrecy rate maximization for intelligent reflecting surface assisted multi-antenna communications," *arXiv*, vol. 23, no. 9, pp. 1488–1492, 2019.

[5] X. Yu, D. Xu, and R. Schober, "Enabling secure wireless communications via intelligent reflecting surfaces," *arXiv*, pp. 0–5, 2019.

[6] M. Cui, G. Zhang, and R. Zhang, "Secure wireless communication via intelligent reflecting surface," *IEEE Wireless Communications Letters*, vol. 8, no. 5, pp. 1410–1414, 2019.

[7] K. Feng and X. Li, "Physical Layer Security Enhancement Exploiting Intelligent Reflecting Surface," *arXiv*, vol. XX, no. XX, pp. 1–5, 2019.

[8] J. Chen, Y. C. Liang, Y. Pei, and H. Guo, "Intelligent Reflecting Surface: A Programmable Wireless Environment for Physical Layer Security," *IEEE Access*, vol. 7, pp. 82 599–82 612, 2019.

[9] X. Guan, Q. Wu, and R. Zhang, "Intelligent Reflecting Surface Assisted Secrecy Communication: Is Artificial Noise Helpful or Not?" *Communication Letters*, vol. 9, no. 6, pp. 778–782, 2020.

[10] W. Wang, H. Tian, W. Ni, and M. Hua, "Intelligent reflecting surface aided secure UAV communications," *arXiv*, vol. 9, no. 1, pp. 108–112, 2020.

[11] N. Hehao and L. Ni, "Intelligent Reflect Surface Aided Secure Transmission in MIMO Channel With SWIPT," *IEEE Access*, vol. 8, pp. 192 132–192 140, 2020.

[12] S. Hong, C. Pan, H. Ren, K. Wang, K. K. Chai, and A. Nallanathan, "Robust transmission design for intelligent reflecting surface aided secure communication systems with imperfect cascaded CSI," *arXiv*, vol. 14, no. 8, 2020.

[13] H.-m. Wang, J. Bai, and L. Dong, "Intelligent Reflecting Surfaces Assisted Secure Transmission Without Eavesdropper's CSI," *IEEE Signal Processing Letters*, vol. 27, pp. 1300–1304, 2020.

[14] B. He, S. Yan, X. Zhou, and V. K. Lau, "On covert communication with noise uncertainty," *IEEE Communications Letters*, vol. 21, no. 4, pp. 941–944, 2017.

[15] Z. Liu, J. Liu, Y. Zeng, and J. Ma, "Covert Wireless Communication in IoT Network: From AWGN Channel to THz Band," *IEEE Internet of Things Journal*, vol. 7, no. 4, pp. 3378–3388, 2020.

[16] X. Lu, E. Hossain, T. Shafique, S. Feng, H. Jiang, and D. Niyato, "Intelligent reflecting surface (IRS)-enabled covert communications in wireless networks," *arXiv*, no. October, pp. 148–155, 2019.

[17] X. Zhou, S. Yan, Q. Wu, F. Shu, and D. W. K. Ng, "Intelligent Reflecting Surface (IRS)-Aided Covert Wireless Communication with Delay Constraint," *arXiv*, no. November, 2020.

[18] X. Lu, E. Hossain, T. Shafique, S. Feng, H. Jiang, and D. Niyato, "Intelligent Reflecting Surface Enabled Covert Communications in Wireless Networks," *IEEE Network*, vol. 34, no. 5, pp. 148–155, 2020.

[19] J. Si, Z. Li, J. Cheng, L. Guan, J. Shi, and N. Al-Dhahir, "Covert Transmission Assisted by Intelligent Reflecting Surface," *arXiv*, pp. 1–30, 2020.

[20] M. Forouzesh, P. Azmi, N. Mokari, K. K. Wong, and D. Goeckel, "Information-theoretic security or covert communication," *arXiv*, no. 1, pp. 1–4, 2018.

[21] R. Sun, B. Yang, Y. Shen, and X. Jiang, "On the Secrecy Capacity of Covert Communication in Full-duplex Relay System," *PLAS*, pp. 26–31, 2020.

[22] M. Forouzesh, P. Azmi, A. Kuhestani, and P. L. Yeoh, "Joint Information Theoretic Secrecy and Covert Communication in the Presence of an Untrusted User and Warden," *arXiv*, pp. 1–9, 2020.

[23] H. M. Wang, Y. Zhang, X. Zhang, and Z. Li, "Secrecy and covert communications against UAV surveillance via multi-hop networks," *IEEE Trans. on Communications*, vol. 68, no. 1, pp. 389–401, 2019.

[24] Q. Wu and R. Zhang, "Intelligent Reflecting Surface Enhanced Wireless Network via Joint Active and Passive Beamforming," *IEEE Trans. on Wireless Communications*, vol. 18, no. 11, pp. 5394–5409, 2019.

[25] Z. Q. Luo, W. K. Ma, A. So, Y. Ye, and S. Zhang, "Semidefinite relaxation of quadratic optimization problems," *IEEE Signal Processing Magazine*, vol. 27, no. 3, pp. 20–34, 2010.

[26] Y. Pei, Y. C. Liang, L. Zhang, K. C. Teh, and K. H. Li, "Secure communication over MISO cognitive radio channels," *IEEE Trans. on Wireless Communications*, vol. 9, no. 4, pp. 1494–1502, 2010.